

Cerium Oxide Nanoparticles Alleviate Neuropathic Pain by Modulating Macrophage Polarization in a Rat SCI Model

Dexiang Ban^{1,2,*}, Hao Yu^{1,2,*}, Zhenyang Xiang^{1,2,*}, Chao Li^{1,2}, Peng Yu^{1,2}, Jianhao Wang^{1,2}, Yang Liu^{1,2}

¹Department of Orthopaedic, Tianjin Medical University General Hospital, Tianjin, 300052, People's Republic of China; ²International Science and Technology Cooperation Base of Spinal Cord Injury, Tianjin Key Laboratory of Spine and Spinal Cord Injury, Department of Orthopedics, Tianjin Medical University General Hospital, Tianjin, 300052, People's Republic of China

*These authors contributed equally to this work

Correspondence: Yang Liu, Department of Orthopaedic, Tianjin Medical University General Hospital, Anshan Road No. 154, Heping District, Tianjin, 300052, People's Republic of China, Email liuyangda66@163.com

Context: Chronic neuropathic pain (NP) frequently occurs after spinal cord injury (SCI) but lacks effective therapeutic options in the clinic. Numerous evidence indicates the involvement of macrophages activation in the NP, and the modulation of macrophages is promising for NP treatment. In this study, we introduce Cerium oxide nanoparticles (CONPs) and aim to investigate whether it can relieve the NP by modulating macrophage polarization.

Methods: CONPs were prepared using the hydrothermal method. In vitro, different concentrations of CONPs were used to cultivate macrophages (RAW 264.7). In vivo, the analgesic effect of CONPs was investigated in a contusive rat SCI model. Mechanical paw withdrawal threshold (PWT) and thermal paw withdrawal latency (PWL) were tested to evaluate pain behaviors. Immunofluorescence staining and real-time quantitative polymerase chain reaction were applied to assess macrophage phenotypes.

Results: The synthesized CONPs were 6.8 ± 0.5 nm in size, presenting a cubic morphology. Live/dead staining showed that the relatively low concentrations of CONPs (less than 800 $\mu\text{g/mL}$) displayed good biocompatibility with macrophages. Intrathecal injection of CONPs could significantly increase the mechanical PWT and thermal PWL of SCI rats. Molecular experiments results showed the expression of M2 macrophage-related markers (CD206, Arg-1, IL-10) were significantly increased, while that of M1 macrophage-related markers (CD86, TNF- α , iNOS) were downregulated after CONPs treatment.

Conclusion: Our study suggests that CONPs can relieve the NP following SCI by promoting M2 macrophages polarization, which provides a novel insight for the treatment of SCI induced NP.

Keywords: cerium oxide nanoparticles, spinal cord injury, neuropathic pain, neuroimmune, macrophages polarization

Introduction

Nearly 68% of the patients with spinal cord injury (SCI) will develop chronic neuropathic pain (NP). The pain can lead to anxiety, depression, and sleep disturbance, greatly reducing the patient's quality of life and increasing the risk of suicide.^{1,2} Instead of recovering their walking abilities, the priority of many SCI patients is relieving the NP. However, this need is largely unmet in the clinic. The existing therapeutic strategies usually behave poorly and are often accompanied by some side effects.³ Therefore, it is necessary to explore more effective interventions for SCI-induced NP management.

Many studies have highlighted the importance of the neuroimmune mechanism underlying NP pathogenesis. The persistent interactions between the immune and nervous systems trigger neuroinflammation, eliciting ectopic neuronal activity and resulting in the NP.^{4,5} Macrophages are the main immune cells and have a significant function in mediating neuroinflammation. They are highly plastic and can polarize into the classical phenotype (M1) and the alternative

phenotype (M2). M1 macrophages can exacerbate the inflammatory responses while M2 macrophages pose anti-inflammatory properties. Modulating the polarization of the macrophage can greatly influence the inflammation processes and has been seen as a promising strategy for NP treatment.^{6–8}

Cerium oxide nanoparticles (CONPs) are redox-active rare earth nanomaterials. It has shown many fascinating biological properties such as anti-inflammation, anti-oxidation, anti-tumor, as well as free radical scavenging, and attracts increased interest for therapeutic application.^{9–12} Some studies have reported the analgesic effect of CONPs in the animal model of spinal nerve injury and diabetic neuropathy.^{13,14} Recently, a study revealed that CONPs could alleviate nociceptive behaviors by inhibiting macrophage activation in the injured sites.¹⁵ The further molecular analysis indicated that after CONPs injection, the cytokines secreted by M1 macrophages were greatly decreased while that of M2 macrophages were upregulated, suggesting CONPs might modulate macrophage polarization in attenuating the NP.^{9,15,16} Based on a series of reports that highlighted the ability of CONPs in relieving the pain and the role of macrophages played in this process, we hypothesize that CONPs can also attenuate the NP after SCI by modulating macrophage polarization. In this study, we prepared nanoceria using the hydrothermal method first. To test this hypothesis, *in vitro*, we used macrophage RAW 264.7 cell lines and *in vivo*, we adopted the SCI contusive rats' model.

Materials and Methods

Particle's Preparation

The nanoceria was synthesized using the hydrothermal process with cerium nitrate hexahydrate ($\text{Ce}(\text{NO}_3)_3 \cdot 6\text{H}_2\text{O}$) as a cerium source. The detailed procedures have been described in the previous report.¹⁷ Controlling the base concentration and reaction temperature, the nanoceria with different sizes and shapes can be obtained. Then, the synthetic nanoceria underwent extensive characterization before the biological experiment. The particle size and shape were evaluated by Transmission Electron microscopy (TEM; Philips Tecnai 10, Amsterdam, The Netherlands). X-ray diffraction (XRD; Bruker advance D8, Germany) was used to characterize crystal morphology and structure. X-ray photoelectron spectroscopy (XPS; Thermo Fisher Scientific, Loughborough, UK) was used to assess qualitatively and quantitatively the surface amount of Ce^{3+} and Ce^{4+} . For cell and animal studies, the prepared nanoceria was firstly dispersed in a cell culture medium at a concentration of 1 mg/mL. The hydrodynamic size and surface electrical properties of dispersions were characterized by dynamic light scattering and Z-potential measurement (DLS; Malvern, Worcestershire, UK).

Cell Culture and Treatment

The RAW 264.7 were purchased from Stem Cell Bank (Chinese Academy of Sciences), and then cultured in Dulbecco's modified Eagle's medium (DMEM; C11330500BT, Gibco) supplemented with 10% fetal bovine serum (FBS; 10100147, Gibco) and 1% penicillin/streptomycin (PS; 15070063, Gibco). A Live/dead assay was performed to evaluate cell viability. Briefly, after 48-h incubation with CONPs, the medium was removed and the samples were stained using LIVE/DEAD™ Viability/Cytotoxicity Kit (L3224, Invitrogen) according to the manufacturer's protocol. The live cells were stained with Calcein AM in green and the dead cells were stained with ethidium homodimer-1 (EthD-1) in red. The images were observed under a fluorescence microscope. For the quantification of cell viability, five images were randomly selected in each group and analyzed using ImageJ software (1.49 V, National Institutes of Health, Bethesda, MD).

RAW were seeded in a 24-well plate at the concentration of 1×10^5 per well and polarized to M1 phenotype via additionally giving supplements of 200 ng/mL lipopolysaccharide (LPS; L2880, Sigma-Aldrich) + 2.5 ng/mL Interferon- γ (IFN- γ ; I3275, Sigma-Aldrich) in the medium. After culturing for 24 hours, different concentrations of CONPs (100 $\mu\text{g}/\text{mL}$ and 200 $\mu\text{g}/\text{mL}$) were added. To detect the impact of CONPs on macrophage phenotype, immunofluorescence staining was applied.

Animals

Adult female Wistar rats (180–250 g) were obtained from SPF (Beijing) Biotechnology Co., Ltd (permission number: SCX (JING) 2019–0010). The rats were group-housed 2–3 per cage and maintained with a 12-h light/dark cycle (light at

7 a.m.) under a temperature and humidity-controlled environment. All animals were given free access to food and water and acclimated for at least 7 days before the surgery for the adaptation to the environment. The experiments were approved by the Animal Ethical and Welfare Committee of Kangtai Medical Laboratory Services Hebei Co., LTD (approval no. MDL20210812-1). All procedures involving animals complied with the National Research Council's Guide for the Care and Use of Laboratory Animals.

Spinal Cord Injury

An established spinal cord contusion injury-induced neuropathic pain model was adopted.^{18,19} After anesthesia satisfaction, the T10 laminectomy was performed and the adjacent spinous process of T9 and T11 were clamped to stabilize the spinal column. The rats were then transferred to the New York University Impactor device (NYU) machine and the exposed spinal T10 segment was contused using a 10 g bob falling from a height of 25 cm. The rats were observed with two hindlimbs twitching involuntarily and the tails wagging which was in accordance with the criteria of spinal cord contusion injury. Then the incision was closed and the rats were kept warm until they woke. The rats' bladders were manually expressed twice a day until the urinary function recovered. The antibiotics (penicillin, 40,000 u/kg/d) were also given to prevent postoperative infection.

Behavioral Tests

The Basso-Beattie-Bresnahan (BBB) scoring system was used to evaluate hindlimb motor function by three independent observers who were blinded to the rats' identity and scored according to standard principles as described by Basso et al. BBB is a 21-point scale locomotion test with 21 indicative of normal movement and 0 representatives of no movement.²⁰

Paw withdrawal threshold (PWT) measured by Von Frey (VF) filaments test was used to describe mechanical hypersensitivity. Briefly, the animals were acclimated for 30 min in plastic cages on the raised metal mesh floor for habituation prior to the pain test. Various VF filaments (RWD Life Science, China) with increased forces (0.4–60 g) were serially applied to the center of the plantar surface of the hind paws (up-down method).²¹ The sudden paw withdrawal was recorded as a positive response and the withdrawal threshold was defined as the lowest bending force of VF that elicited the positive responses.

Paw withdrawal latency (PWL) examined by the Hargreaves test was used to evaluate the heat sensitivity.²² Similarly, after acclimation for 30 minutes on a glass plate covered with a transparent chamber, infrared heat stimulation with a moveable radiant thermal source (RWD Life Science, China) was exerted on the center of the plantar surface. The heat intensity was set to produce basal PWL of approximately 12s, with the cut-off criteria of 20s in case of tissue damage. Each hind limb paw was tested 5 times at 10 min intervals and the final PWL for each rat was averaged.

The locomotion test and pain behavioral test were performed 4 weeks after SCI to ensure the success of establishing SCI induced central neuropathic pain model.²³ After CONPs treatment, the behavioral tests were performed for another week to evaluate the efficacy of CONPs treatment.

Intrathecal Injection

To establish the homogenous animal models, we first selected those rats with BBB scores of 8–9 the 28 days after SCI. Then, we selected those rats which developed neuropathic pain after SCI with the criteria of PWT around 2–3 g and PWL around 5–6 s. Most rats (35/40) met the criteria and were included in the following experiment. Then, they were grouped as follows:

- Group 1: Vehicle group (n = 10).
- Group 2: CONPs 0.5 mg/mL group (n = 10).
- Group 3: CONPs 1 mg/mL group (n = 10).

The intrathecal injection was performed via direct lumbar puncture using a 30 μ L Hamilton syringe (26-G needle, Reno, NV, USA) as previously described.²⁴ A sudden tail-flick suggested that the needle arrived at the appropriate site. The vehicle group received the intrathecal injection of 20 μ L PBS at one time. CONPs were prepared at 0.5 mg/mL and

1 mg/mL in PBS by sonicating for 5 min, the doses of which were based on the previous report.¹⁶ Then, CONPs (0.5 and 1 mg/mL) with the same volume of 20 μ L were performed intrathecal injection respectively.

Sample Collection

One week post-treatment, the rats were sacrificed and intracardially perfused with 150 mL pre-cold PBS followed by 100 mL paraformaldehyde (PFA; 4% w/v). Approximately 10 mm spinal cord containing the injury site was dissected. The spinal cord was fixed in 4% paraformaldehyde overnight and cryoprotected with 30% sucrose for 2 days. For tissue immunostaining, 6 spinal cords in each group were embedded in optimal cutting temperature (OCT) and conducted in serial 10 μ m - thick sagittal sections. The remaining samples were stored at -80°C for molecular work.

Immunofluorescence Staining

After three rinses with PBS, cells and frozen tissues sections were fixed with 4% PFA for 20 min, permeabilized with 0.5% TritonX-100 (85111, Thermo Scientific) for 12 min, and blocked with 5% bovine serum albumin (A1933, Sigma-Aldrich) for 20 min. All performances were at room temperature (RT). Then, cells and fixed sections were incubated overnight at 4°C with primary antibodies: ED1, CD86, and Arg1. The next day, in the dark environment, the cells and samples were incubated with the secondary antibodies (conjugated to DyLight 488 or Cy3) for 1 h and subsequently counterstained with 4',6'-diamidino-2-phenylindole (DAPI; C1002, Beyotime) for the nucleus. The images were observed under inverted fluorescence microscopy (Nikon, Tokyo, Japan). For tissue immunofluorescence staining, macrophage polarization was quantified by calculating the percentage of the bright responses to anti-CD86 and anti-Arg1 antibodies in each section. Five sagittal sections were randomly selected and evaluated using ImageJ software (National Institutes of Health). Detailed information about the antibodies mentioned above can be found in Table 1.

RT-PCR

Total RNA was isolated with TRIzol reagent (R6834-01, Omega) according to the manufacturer's protocol. cDNA was transcribed from total RNA (1 μ g/sample) using the PrimeScript RT reagent kit (5081963001, Roche). Quantitative real-time PCR was performed using FastStart Universal SYBR Green Master (4913850001, Roche) on a Light Cycler[®] 480Real-Time PCR System (Hoffman-La Roche Ltd., Basel, Switzerland). The conditions were set as follows: 95°C for 10 min followed by 40 cycles of 95°C for 15s and 60°C for the 60s. The expression levels of each target gene were normalized to GAPDH (internal control) and the relative expression levels of target genes in experiment groups to that in the vehicle group were calculated with the $2^{-\Delta\Delta\text{CT}}$ method. All the primers used were listed in Table 2.

Statistical Analysis

All data analyses were performed using GraphPad Prism 8. A pairwise comparison was made using Student's *t*-test. The comparison between multiple groups was made by one-way analysis of variance (ANOVA), followed by Turkey's multiple comparisons as the post hoc test to determine the difference between the two groups. $P < 0.05$ was considered significant. The data were shown in mean \pm standard deviation (SD).

Table 1 A Summary of Antibodies Used for Immunostaining

Antibodies	Sources	Dilution	Identifier
Anti-mouse ED1	Thermo Fisher	1:200	MA5-16654
Anti-rabbit CD86	Thermo Fisher	1:200	PA5-88284
Anti-rabbit Arg1	Abcam	1:200	ab96183
Goat anti-mouse IgG (DyLight 488)	Boster	1:100	BA1126
Goat anti-rabbit IgG (DyLight 488)	Boster	1:100	BA11127
Goat anti-rabbit IgG (Cy3)	Boster	1:100	BA1032

Table 2 Primers Used for RT-qPCR

Gene	Primer Sequence
GAPDH	F: 5'-CCCTTAAGAGGGATGCTGCC-3' R: 5'-TACGGCCAAATCCGTTTACA-3'
TNF- α	F: 5'-CTGAACTTCGGGGTATCGG-3' R: 5'-GGCTTGCTACTCGAATTTTGAGA-3'
iNOS	F: 5'-TGGTGAAGGGACTGAGCTGT-3' R: 5'-CTGAGAACAGCACAAGGGGT-3'
IL-1 β	F: 5'-TGGAGAGTGTGGATCCCAAG-3' R: 5'-GGTGCTGATGTACCAGTTGG-3'
Arg-1	F: 5'-CACCTGAGTTTTGATGTTGATGG-3' R: 5'-TCCTGAAAGTAGCCCTGTCTTGT-3'
CD206	F: 5'-ACGAGCAGGTGCAGTTTACA-3' R: 5'-ACATCCCATAAGCCACCTGC-3'
IL-10	F: 5'-GAGAAGCATGGCCAGAAATC-3' R: 5'-GAGAAATCGATGACAGCGCC-3'

Results

Characterization of CONPs

The synthetic nanoceria underwent extensive characterization. TEM image exhibited a size ranging 6.8 ± 0.5 nm and the single nanocrystal presented a cubic morphology (Figure 1A–C). No impurities can be detected and CONPs displayed typical peak broadening characteristics of nanosized particles, as determined by XRD analysis (Figure 1D). The bioactivity of CONPs was greatly based on the electron transfer between Ce^{3+} and Ce^{4+} . XPS spectra showed the relative level of Ce^{3+} and Ce^{4+} were $27.80 \pm 3.53\%$ and $72.19 \pm 3.52\%$ respectively, which ensures the catalytic activity of CONPs (Figure 1E).²⁵ To characterize the actual size of CONPs in biological tests, DLS analysis was performed and the results showed the hydrodynamic size of CONPs increased to 74.5 nm, suggesting nanoceria might assemble in a culture medium (Figure 1F). The measured Z-potential was + 18.2 mv which might be attributed to the presence of cationic on its surface (Figure 1G).

In vitro CONPs Modulate Macrophage Polarization

Before exploring the abilities that nanoceria might have on transforming macrophage phenotype, it was imperative to evaluate its cytotoxic effect. We performed a live/dead staining assay and the results revealed that a high dosage of CONPs application (800 $\mu\text{g/mL}$) would reduce macrophage viability (Figure 2A and B, $P < 0.001$, $F = 20.02$). Thus, nanoceria solutions with relatively low concentrations were used in the following in vitro study.

To examine the effects of CONPs on macrophage phenotype, we performed immunofluorescence staining. For immunofluorescence staining, cells were stained with CD86 (an M1 marker) and Arg1 (an M2 marker). The fluorescence intensity of CD86 displayed the trends as follows: M1 > M1+ CONPs (200 $\mu\text{g/mL}$) > M1+ CONPs (400 $\mu\text{g/mL}$) > control, and the intensity of Arg1 displayed the trends as follows: M1+ CONPs (400 $\mu\text{g/mL}$) > M1+ CONPs (200 $\mu\text{g/mL}$) > M1 > control (Figure 2C). Our results suggested that CONPs treatment could increase the percentage of M2 macrophages while reducing that of M1 macrophages.

In vivo CONPs Attenuate Pain Behaviors Following SCI

After spinal cord contusion injury, the rats' hindlimbs were immediately paralyzed but spontaneously recovered within 21 days until BBB scores 8–9 (Figure 3A). The response to the innocuous, mechanical stimuli was not detected until 7 days after SCI and thereafter, the mechanical PWT decreased progressively (Figure 3B). The responsive latency of the injured rats to the thermal stimuli was prolonged compared with the sham group within the 14 days after SCI and thereafter, the thermal PWL decreased gradually (Figure 3C). For the injured rats, there was no response to the highest VF stimuli in the first week and the PWL values were also higher than the sham group within the first two weeks. Both

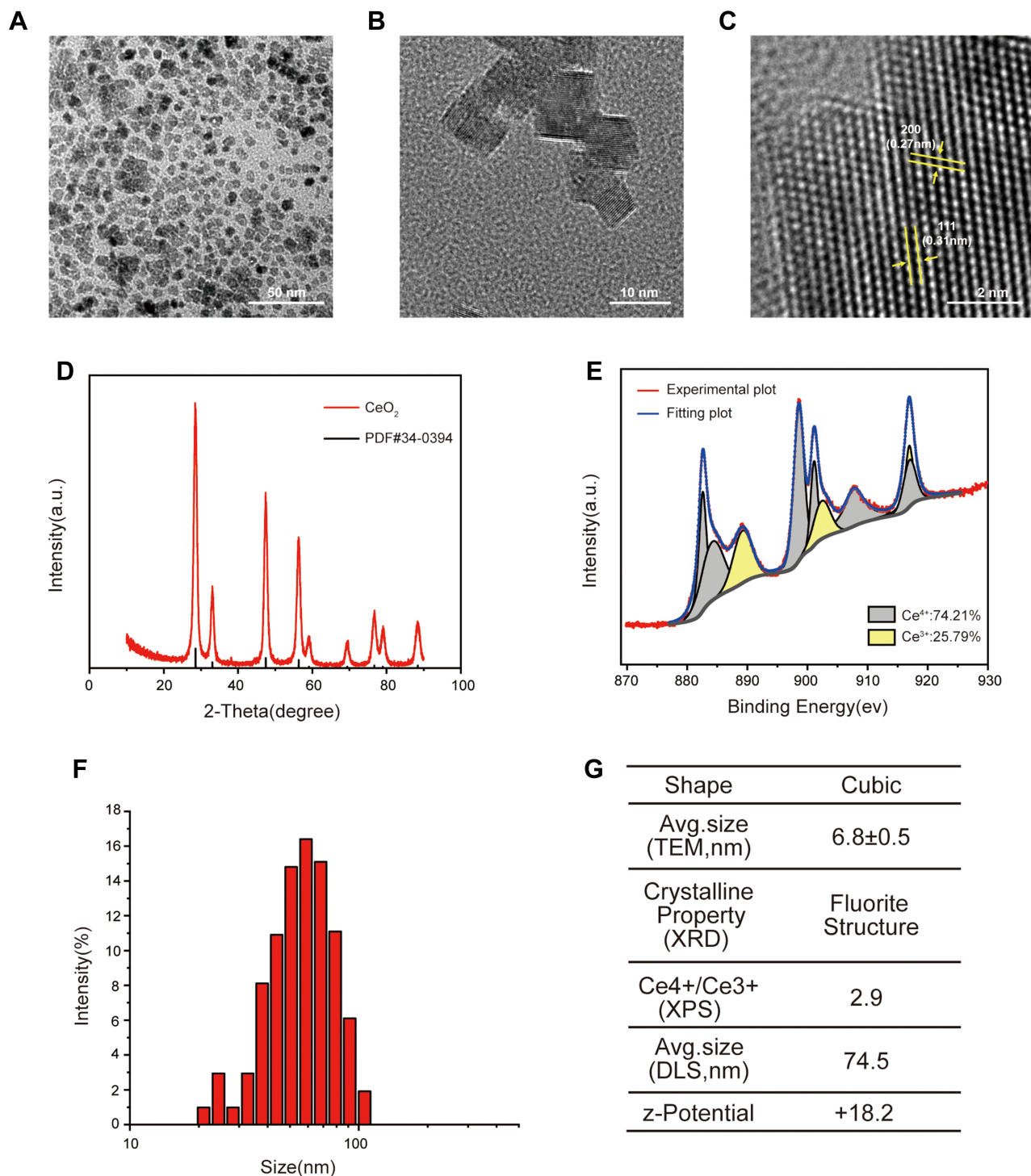


Figure 1 Characteristics of cerium oxide nanoparticles (CONPs). **(A–C)** Transmission electron microscopy (TEM) image of CONPs. Arrows indicate the (111) and (200) lattice fringes with the interplanar spacing of 0.31 nm and 0.27 nm respectively. Scales = 10 nm **(A)**, 50 nm **(B)** and 2 nm **(C)**. **(D)** X-ray diffraction (XRD) pattern of CONPs. **(E)** Representative image of X-ray photoelectron spectroscopy (XPS) spectra of CONPs. **(F)** Dynamic light scattering (DLS) measurement of CONPs. **(G)** Summary of properties of CONPs.

might be attributed to the low level of hindlimb motor function within the first two weeks following surgery. Then, the NP developed from day 14 for mechanical allodynia and from day 21 for thermal hyperalgesia. On day 28 after SCI, the injured rats showed significant mechanical and thermal pain (Figure 3B and C, $P < 0.05$).

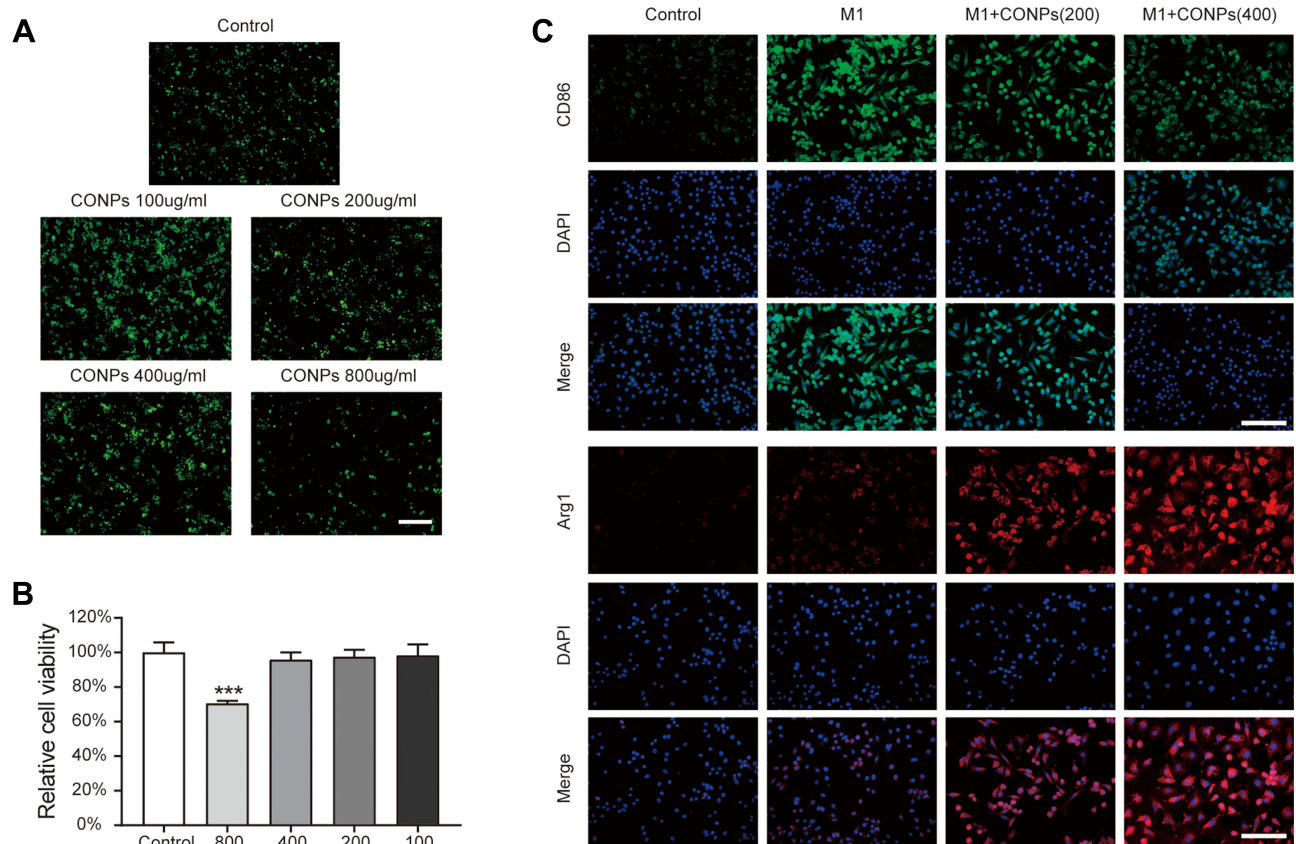


Figure 2 Effects of CONPs on macrophage viability and polarization. **(A and B)** Representative images **(A)** and statistical analysis **(B)** of live/dead staining showed a high concentration of CONPs treatment (800 µg/mL) can decrease the cell viability of macrophages (n = 5 each group). Scale bar = 100 µM. **(C)** Immunofluorescence analysis of macrophage phenotype distribution after CONPs treatment (n = 5 each group). M1 macrophages positive for CD86 (green) and M2 macrophages positive for Arg1 (red). Scale bar = 25 µM. The data were shown in mean ± standard deviation. P < 0.05 was set as significance. Compared with the control group, ***P < 0.001.

To evaluate whether CONPs treatment could attenuate pain behaviors, we delivered CONPs to the injured spinal cord which the NP developed through intrathecal injection. As shown in **Figure 3E and F**, both concentrations of CONPs solution significantly improved the mechanical PWT (F = 66.95; 0.5 mg/mL: P < 0.05; 1 mg/mL: P < 0.05) and thermal PWL compared (F = 29.94; 0.5 mg/mL: P < 0.05; 1 mg/mL: P < 0.05) with the vehicle group. Besides, the SCI rats that received higher concentrations of CONPs displayed better analgesic effects. What's more, the CONPs treatment also improved the hindlimb motor function. The BBB scores increased from 8.3 ± 0.5 to 11.6 ± 0.6 (CONPs, 0.5 mg/mL) and from 8.6 ± 0.6 to 13.5 ± 0.7 (CONPs, 1 mg/mL) in one-week post-injection while the vehicle group did not exhibit any difference (**Figure 3D**).

In vivo, CONPs Nanoparticles Modulate Macrophage Polarization

To explore the underlying mechanism by which the CONPs attenuate the NP, we labeled the macrophages with ED1, M1 macrophages with CD86, and M2 macrophages with Arg1. After CONPs treatment, the CD86⁺/ED1⁺ cells were significantly decreased (F = 137.4; 0.5 mg/mL: P < 0.01; 1 mg/mL: P < 0.01) while the CD206⁺/ED1⁺ cells (F = 52.69; 0.5 mg/mL: P < 0.01; 1 mg/mL: P < 0.01) were significantly increased (**Figure 4A and B**). We also analyzed the mRNA expression in the tissue samples one week after injection treatment. The results showed the expression of M1 markers including IL-1β (F = 17.73; 0.5 mg/mL: P < 0.01; 1 mg/mL: P = 0.0572), TNF-α (F = 142.5; 0.5 mg/mL: P < 0.01; 1 mg/mL: P < 0.01), iNOS (F = 79.32; 0.5 mg/mL: P < 0.01; 1 mg/mL: P < 0.01), and CD86 (F = 65.53; 0.5 mg/mL: P < 0.01; 1 mg/mL: P < 0.01) were reduced (**Figure 4C**). On the other hand, M2 makers including Arg-1 (F = 19.18; 0.5 mg/mL: P < 0.05; 1 mg/mL: P < 0.01) and IL-10 (F = 15.66; 0.5 mg/mL: P < 0.05; 1 mg/mL: P < 0.01) were

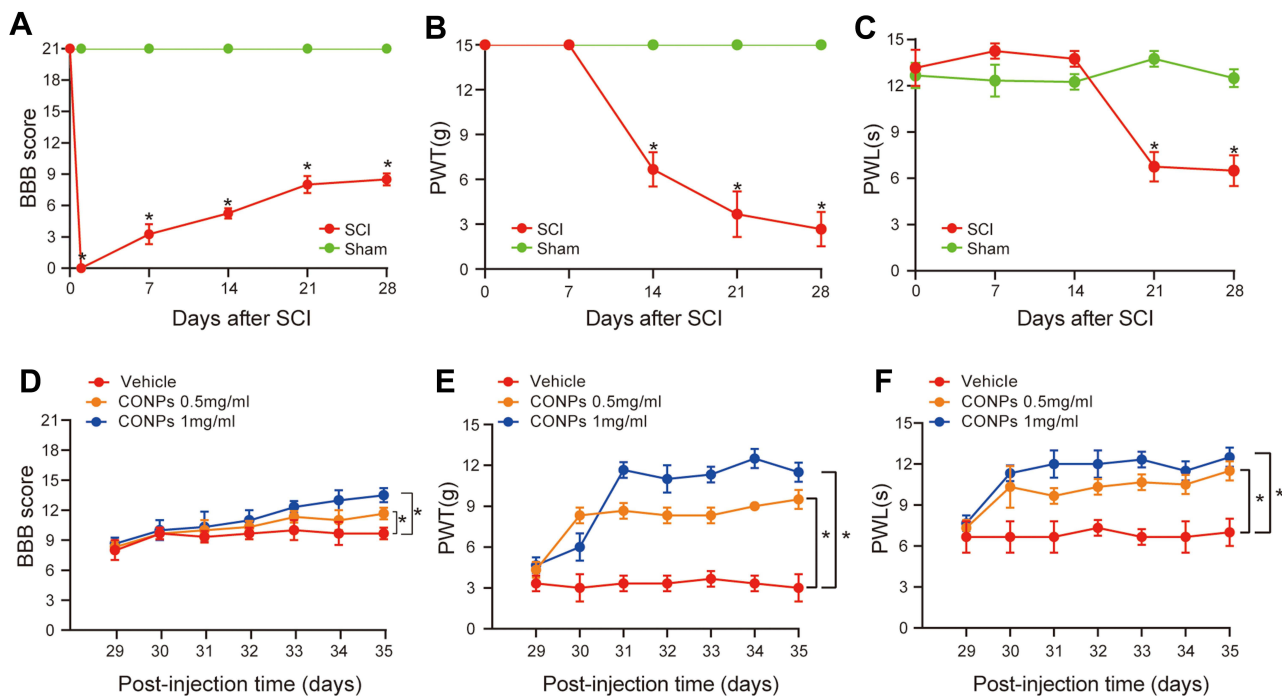


Figure 3 CONPs reduced neuropathic pain after SCI in vivo. **(A)** Motor function was assessed by BBB score after SCI ($n = 40$). **(B and C)** Pain responses to mechanical stimuli **(B, PWT)** and thermal stimuli **(C, PWL)** after SCI ($n = 40$). The SCI rats which developed neuropathic pain received CONPs injection on day 28 post-injury. **(D–F)** Intrathecal injection of CONPs significantly increased the motor function of SCI rats **(D)** and improved their pain responses to mechanical **(E)** and thermal **(F)** stimuli ($n = 10$ each group). The data were shown in mean \pm standard deviation. $P < 0.05$ was set as significance. Compared with the sham or vehicle group, $*p < 0.05$. **Abbreviations:** PWT, paw withdrawal threshold; PWL, paw withdrawal latency.

confirmed to be increased (Figure 4D). Although, there was no significant difference in CD206 among all groups. Collectively, our results suggested that CONPs could promote macrophages' polarization from M1 to M2 after SCI.

Discussion

Many researchers in the SCI region mainly focused on neuron regeneration and motor function recovery while ignoring the assessment of NP. However, NP is frequently complicated with SCI and usually causes depression, and sleep disturbance and seriously compromises patients' life quality.²⁶ In addition, effective treatments for NP are largely in lack in the clinic.²⁷ Thus, it's necessary to examine whether the NP is relieved while exploring new therapeutic methods for SCI repair. Some recent studies reported that nanoceria could repair the injured spinal cord and promote SCI rats' locomotor function recovery.^{16,28} Here, we synthesized CONPs nanoparticles using the hydrothermal method. Besides, we adjusted the base concentration and reaction temperature in hope of getting a smaller nanoceria than that described by Jong-Wan Kim et al.¹⁷ There are mainly two reasons for doing so: first, the smaller particle size of nanoceria ensures a higher concentration of oxygen vacancy on the surface and more active biological activity;²⁹ second, smaller nanoceria displayed better metabolism and biosafety.¹⁰ Then, we established the SCI-induced NP model and injected the nanoceria solution into the injured rats. The motor and sensory functions were assessed and histological analysis was also performed. We found CONPs could modulate macrophage polarization and attenuate pain behaviors following SCI.

Of the various immune cells infiltrating into the sites of nerve injury, macrophages predominate.³⁰ The effects of those macrophages on the development of NP are controversial depending on their different phenotypes: M1 and M2.^{7,31} The damaged nociceptive neurons upregulate the expression of proinflammatory cytokines and chemokines receptors.^{32,33} Thus, M1 macrophages, known for producing large amounts of pro-inflammatory molecules such as IL-6, IL-1 β , and TNF- α , usually elicit the ectopic activity of nociceptors and exacerbate the pain.^{34,35} While M2 macrophages act oppositely, tilting in the direction of inflammation resolution and pain relief.³⁶ Targeted polarization of macrophages from M1 to M2 phenotype has been proved to be effective in reducing NP. For example, Norikazu et al

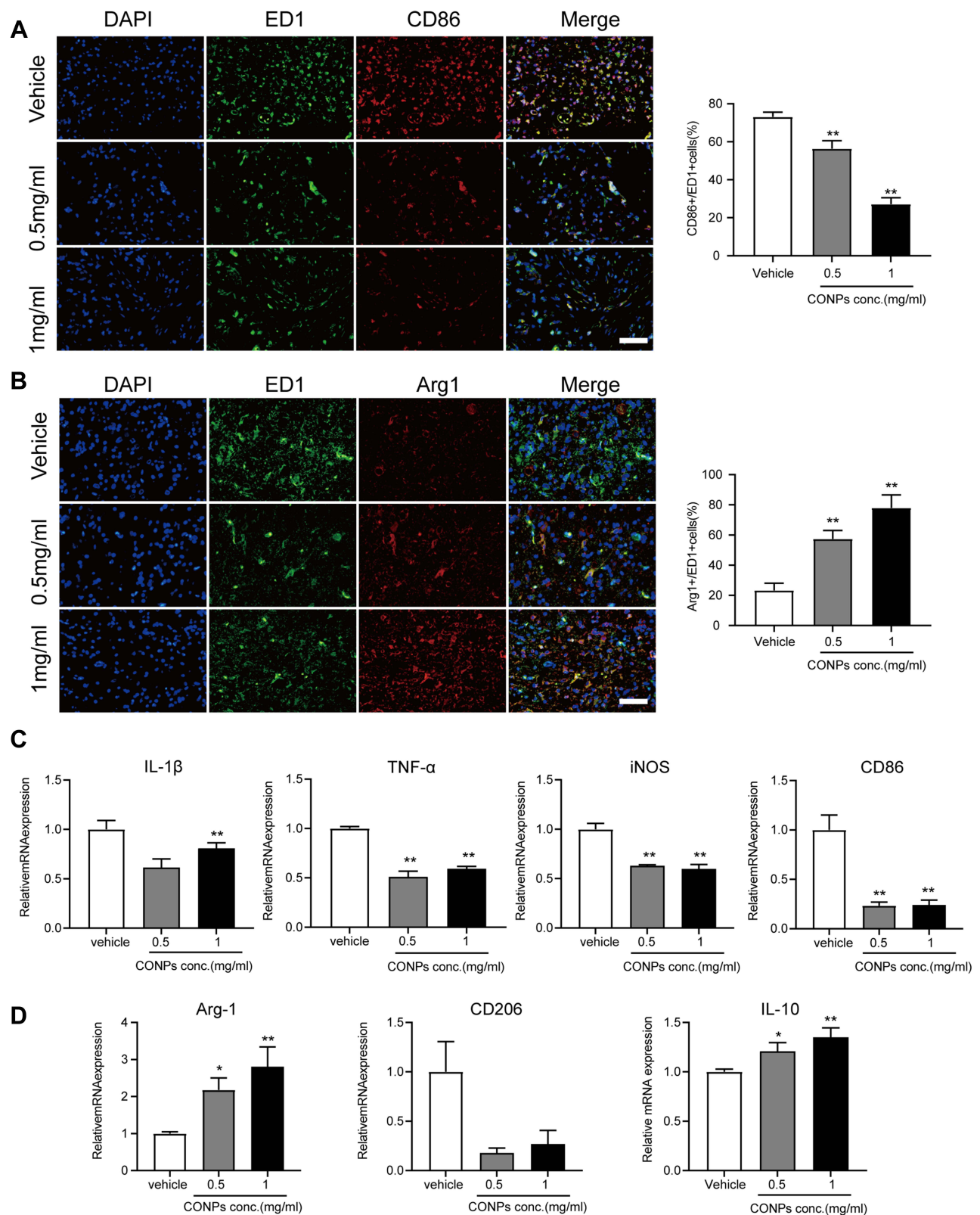


Figure 4 CONPs treatment promoted M2 macrophage polarization. **(A and B)** Representative immunofluorescence image of macrophage phenotype distribution after CONPs treatment (left, n = 12 each group). Scale bar = 50 μ M. M1 macrophages positive for CD86 (red) and M2 macrophages positive for Arg1 (red). Cells were co-stained with pan macrophage markers (ED1, green). Statistical analysis showed CONPs injection significantly increased the percentage of Arg1+/ED1+ cells while decreasing that of CD68+/ED1+ cells (right). **(C)** Gene expression analysis of M1-related markers by qRT-PCR (n = 5 each group). **(D)** Gene expression of M2-related markers by RT-qPCR (n = 5 each group). The data were shown in mean \pm standard deviation. P < 0.05 was set as significance. Compared with the vehicle group, *P < 0.05, **P < 0.01.

injected IL-4 surrounding the mice's injured sciatic nerve to increase the proportion of M2 macrophages and observed a marked reduction of pain behaviors.³⁷ Another study by Hu et al reported red light therapy had a similar effect on recruiting M2 macrophages and relieved the pain condition following SCI.³⁸ In this study, we also tried to increase M2 macrophages in the injured sites and to see whether the NP induced by SCI can be attenuated.

Many studies have implied the ability of CONPs in modulating macrophage polarization. Hirst et al reported the anti-inflammatory properties of nanoceria by regulating inflammatory mediators' production from the macrophages.⁹ Kai-Li et al incorporated CONPs nanoparticles into the hydroxyapatite (HA) to endow it with the ability to transfer macrophages' phenotype from M1 to M2 type, while HA alone would provoke proinflammatory responses.³⁹ Besides, a study about pulmonary inflammation suggests nanoceria was able to reprogram alveolar macrophages (AM) from the M1 to M2 phenotype.⁴⁰ Here, we examined our hypothesis using RAW 264.7 macrophage cell lines. We first cocultured RAW with CONPs under different concentrations and found CONPs with concentrations of 800 µg/mL could markedly lead to the macrophages' cell death. This may explain why some researchers observed the adverse cellular response such as increased cell apoptotic rate and ROS when applying CONPs.^{41,42} The CONPs nanoparticles may work dose-dependent. Next, we evaluated the effect of nanoceria on macrophage phenotype qualitatively. The macrophage-specific markers CD86 and Arg1 were used to identify M1 and M2 phenotypes respectively. The results of immune fluorescence staining suggested that CONPs nanoparticles could significantly increase the percentages of M2 macrophages while decreasing that of M1 macrophages. Interestingly, a higher concentration of nanoceria (400 µg/mL) seems to induce more M2 macrophage polarization. Though, the relationship between the concentration of nanoceria and the phenotypic switch of macrophages requires further study.

Almost 70% study concerning SCI-induced NP adopted the thoracic spinal cord contusion model.⁴³ Researchers assess the pain condition primarily based on the withdrawal responses from the mechanical or thermal stimuli. Because those nociceptive withdrawal reflexes are frequently observed in humans with NP.⁴⁴ In this study, our observation was in line with the literature that rats after spinal cord injury developed significant mechanical hypersensitivity and thermal allodynia as the frequency and latency of paw withdrawal increased.⁴⁵ Through intrathecal injection, we administered CONPs intervention on those animals with NP. In the following week, we found the rats' motor function significantly improved which was consistent with previous studies.²⁸ In addition, the mechanical PWT and thermal PWL were increased, suggesting that CONPs possess a pain-relieve effect. Some recent studies have implicated the analgesia effect of CONPs in various animal models. For example, Kim et al reported that CONPs could alleviate edema and pain hypersensitivity in the animal model of inflammation pain.¹⁵ Therefore, these findings in the present study were in accordance with previous studies and implied that the use of nanoceria for pain relief was worthy of further study.

We also evaluated the effect of CONPs on macrophage polarization *in vivo*. Both tissue immunostaining and qRT-PCR displayed a similar changing trend of M1/M2 macrophages. Interestingly, Jong-Wan Kim et al reported the optimal therapeutic dosage of nanoceria in treating SCI was between 0.5 –1 mg/mL and we adopted the concentration they reported.¹⁶ However, our study suggested the optimal concentration of nanoceria in treating SCI-induced NP may be higher than 1 mg/mL. Because the *in vivo* study seemed to present a trend that the higher concentration of CONPs treatment leads to more M2 macrophage polarization and better analgesic effect. Besides, in neuropathic pain, M1 macrophages activation is known to elevate the sensitivity of somatosensory neurons by secreting large quantities of pro-inflammatory cytokines and further enhance NP, while there is ample evidence suggesting phenotypic transfer of M2 macrophages can diminish nerve injury-induced mechanical hypersensitivity.^{46–48} The present study revealed that CONPs injection could significantly increase the proportion of M2 macrophages and decrease that of M1 macrophages. Based on those observations, we speculated the analgesia of CONPs could be attributed to its modulation effect in macrophage subtypes.

Conclusion

Overall, the present study demonstrated that CONPs could alleviate neuropathic pain after rats' SCI by promoting macrophage polarization towards M2 phenotypes. In addition, CONPs could also promote motor function recovery in rats' SCI model. Thus, our findings implied the great pharmaceutical application of CONPs in treating SCI-induced neuropathic pain.

Acknowledgments

This work was supported by grants from the National Natural Science Foundation of China (81972061, 81871766).

Disclosure

The authors report no conflicts of interest in this work.

References

1. Shiao R, Lee-Kubli C. Neuropathic pain after spinal cord injury: challenges and research perspectives. *Neurotherapeutics*. 2018;15(3):635–653. doi:10.1007/s13311-018-0633-4
2. Burke D, Fullen B, Stokes D, Lennon O. Neuropathic pain prevalence following spinal cord injury: a systematic review and meta-analysis. *Eur J Pain*. 2017;21(1):29–44. doi:10.1002/ejp.905
3. Widerström-Noga E, Turk D. Types and effectiveness of treatments used by people with chronic pain associated with spinal cord injuries: influence of pain and psychosocial characteristics. *Spinal Cord*. 2003;41(11):600–609. doi:10.1038/sj.sc.3101511
4. Lim J, Kam P. Neuroimmune mechanisms of pain: basic science and potential therapeutic modulators. *Anaesth Intensive Care*. 2020;48(3):167–178. doi:10.1177/0310057X20902774
5. Ellis A, Bennett D. Neuroinflammation and the generation of neuropathic pain. *Br J Anaesth*. 2013;111(1):26–37. doi:10.1093/bja/aet128
6. Hirokawa N, Uchida K, Kuniyoshi K, et al. Vein wrapping promotes M2 macrophage polarization in a rat chronic constriction injury model. *J Orthop Res*. 2018;36(8):2210–2217. doi:10.1002/jor.23875
7. Kiguchi N, Kobayashi D, Saika F, Matsuzaki S, Kishioka S. Pharmacological regulation of neuropathic pain driven by inflammatory macrophages. *Int J Mol Sci*. 2017;18(11):11. doi:10.3390/ijms18112296
8. Kalynovska N, Diallo M, Sotakova-Kasparova D, Palecek J. Losartan attenuates neuroinflammation and neuropathic pain in paclitaxel-induced peripheral neuropathy. *J Cell Mol Med*. 2020;24(14):7949–7958. doi:10.1111/jcmm.15427
9. Hirst S, Karakoti A, Tyler R, Sriranganathan N, Seal S, Reilly C. Anti-inflammatory properties of cerium oxide nanoparticles. *Small*. 2009;5(24):2848–2856. doi:10.1002/sml.200901048
10. Bao Q, Hu P, Xu Y, et al. Simultaneous blood-brain barrier crossing and protection for stroke treatment based on edaravone-loaded ceria nanoparticles. *ACS nano*. 2018;12(7):6794–6805. doi:10.1021/acsnano.8b01994
11. Xiao Y, Li J, Wang S, et al. Cerium oxide nanoparticles inhibit the migration and proliferation of gastric cancer by increasing DHX15 expression. *Int J Nanomedicine*. 2016;11:3023–3034. doi:10.2147/IJN.S103648
12. Ciofani G, Genchi G, Liakos I, et al. Effects of cerium oxide nanoparticles on PC12 neuronal-like cells: proliferation, differentiation, and dopamine secretion. *Pharm Res*. 2013;30(8):2133–2145. doi:10.1007/s11095-013-1071-y
13. Najafi R, Hosseini A, Ghaznavi H, Mehrzadi S, Sharifi A. Neuroprotective effect of cerium oxide nanoparticles in a rat model of experimental diabetic neuropathy. *Brain Res Bull*. 2017;131:117–122. doi:10.1016/j.brainresbull.2017.03.013
14. Choi B, Soh M, Manandhar Y, et al. Highly selective microglial uptake of ceria-zirconia nanoparticles for enhanced analgesic treatment of neuropathic pain. *Nanoscale*. 2019;11(41):19437–19447. doi:10.1039/C9NR02648G
15. Kim J, Hong G, Mazaleuskaya L, et al. Ultrasmall antioxidant cerium oxide nanoparticles for regulation of acute inflammation. *ACS Appl Mater Interfaces*. 2021;13(51):60852–60864. doi:10.1021/acsmi.1c16126
16. Kim J, Mahapatra C, Hong J, et al. Functional recovery of contused spinal cord in rat with the injection of optimal-dosed cerium oxide nanoparticles. *Adv Sci*. 2017;4(10):1700034. doi:10.1002/advs.201700034
17. Mai H, Sun L, Zhang Y, et al. Shape-selective synthesis and oxygen storage behavior of ceria nanopolyhedra, nanorods, and nanocubes. *J Phys Chem B*. 2005;109(51):24380–24385. doi:10.1021/jp055584b
18. Ban D, Ning G, Feng S, et al. Combination of activated Schwann cells with bone mesenchymal stem cells: the best cell strategy for repair after spinal cord injury in rats. *Regen Med*. 2011;6(6):707–720. doi:10.2217/rme.11.32
19. Zhao C, Zhou T, Zhao X, et al. Delayed administration of nafamostat mesylate inhibits thrombin-mediated blood-spinal cord barrier breakdown during acute spinal cord injury in rats. *J Neuroinflammation*. 2022;19(1):189. doi:10.1186/s12974-022-02531-w
20. Basso D, Beattie M, Bresnahan J. A sensitive and reliable locomotor rating scale for open field testing in rats. *J Neurotrauma*. 1995;12(1):1–21. doi:10.1089/neu.1995.12.1
21. Chaplan S, Bach F, Pogrel J, Chung J, Yaksh T. Quantitative assessment of tactile allodynia in the rat paw. *J Neurosci Methods*. 1994;53(1):55–63. doi:10.1016/0165-0270(94)90144-9
22. Lee J, Choi D, Oh T, Yune T, Costigan M. Analgesic effect of acupuncture is mediated via inhibition of JNK activation in astrocytes after spinal cord injury. *PLoS One*. 2013;8(9):e73948. doi:10.1371/journal.pone.0073948
23. Lee J, Choi H, Ju B, Yune T. Estrogen alleviates neuropathic pain induced after spinal cord injury by inhibiting microglia and astrocyte activation. *Biochim Biophys Acta Mol Basis Dis*. 2018;1864(7):2472–2480. doi:10.1016/j.bbadis.2018.04.006
24. Mestre C, Pélissier T, Fialip J, Wilcox G, Eschalier A. A method to perform direct transcutaneous intrathecal injection in rats. *J Pharmacol Toxicol Methods*. 1994;32(4):197–200. doi:10.1016/1056-8719(94)90087-6
25. Celardo I, De Nicola M, Mandoli C, Pedersen J, Traversa E, Ghibelli L. Ce³⁺ ions determine redox-dependent anti-apoptotic effect of cerium oxide nanoparticles. *ACS nano*. 2011;5(6):4537–4549. doi:10.1021/nn200126a
26. Finnerup N. Neuropathic pain and spasticity: intricate consequences of spinal cord injury. *Spinal Cord*. 2017;55(12):1046–1050. doi:10.1038/sc.2017.70
27. Widerström-Noga E. Neuropathic pain and spinal cord injury: phenotypes and pharmacological management. *Drugs*. 2017;77(9):967–984. doi:10.1007/s40265-017-0747-8
28. Behroozi Z, Rahimi B, Hamblin M, Nasirinezhad F, Janzadeh A, Ramezani F. Injection of cerium oxide nanoparticles to treat spinal cord injury in rats. *J Neuropathol Exp Neurol*. 2022;81(8):635–642. doi:10.1093/jnen/nlac026

29. Celardo I, Pedersen J, Traversa E, Ghibelli L. Pharmacological potential of cerium oxide nanoparticles. *Nanoscale*. 2011;3(4):1411–1420. doi:10.1039/c0nr00875c
30. Popovich P, Guan Z, Wei P, Huitinga I, van Rooijen N, Stokes B. Depletion of hematogenous macrophages promotes partial hindlimb recovery and neuroanatomical repair after experimental spinal cord injury. *Exp Neurol*. 1999;158(2):351–365. doi:10.1006/exnr.1999.7118
31. Kiguchi N, Sakaguchi H, Kadowaki Y, et al. Peripheral administration of interleukin-13 reverses inflammatory macrophage and tactile allodynia in mice with partial sciatic nerve ligation. *J Pharmacol Sci*. 2017;133(1):53–56. doi:10.1016/j.jphs.2016.11.005
32. Ji R, Chamesian A, Zhang Y. Pain regulation by non-neuronal cells and inflammation. *Science*. 2016;354(6312):572–577. doi:10.1126/science.aaf8924
33. Ren K, Dubner R. Interactions between the immune and nervous systems in pain. *Nat Med*. 2010;16(11):1267–1276. doi:10.1038/nm.2234
34. Nicol G, Lopshire J, Pafford C. Tumor necrosis factor enhances the capsaicin sensitivity of rat sensory neurons. *J Neurosci*. 1997;17(3):975–982. doi:10.1523/JNEUROSCI.17-03-00975.1997
35. Obreja O, Rathee P, Lips K, Distler C, Kress M. IL-1 beta potentiates heat-activated currents in rat sensory neurons: involvement of IL-1RI, tyrosine kinase, and protein kinase C. *FASEB j*. 2002;16(12):1497–1503. doi:10.1096/fj.02-0101com
36. Kigerl K, Gensel J, Ankeny D, Alexander J, Donnelly D, Popovich P. Identification of two distinct macrophage subsets with divergent effects causing either neurotoxicity or regeneration in the injured mouse spinal cord. *J Neurosci*. 2009;29(43):13435–13444. doi:10.1523/JNEUROSCI.3257-09.2009
37. Kiguchi N, Kobayashi Y, Saika F, Sakaguchi H, Maeda T, Kishioka S. Peripheral interleukin-4 ameliorates inflammatory macrophage-dependent neuropathic pain. *Pain*. 2015;156(4):684–693. doi:10.1097/j.pain.0000000000000097
38. Hu D, Zhu S, Potas J. Red LED photobiomodulation reduces pain hypersensitivity and improves sensorimotor function following mild T10 hemiconfusion spinal cord injury. *J Neuroinflammation*. 2016;13(1):200. doi:10.1186/s12974-016-0679-3
39. Li K, Shen Q, Xie Y, You M, Huang L, Zheng X. Incorporation of cerium oxide into hydroxyapatite coating regulates osteogenic activity of mesenchymal stem cell and macrophage polarization. *J Biomater Appl*. 2017;31(7):1062–1076. doi:10.1177/0885328216682362
40. Ma J, Zhao H, Mercer R, et al. Cerium oxide nanoparticle-induced pulmonary inflammation and alveolar macrophage functional change in rats. *Nanotoxicology*. 2011;5(3):312–325. doi:10.3109/17435390.2010.519835
41. Park E, Choi J, Park Y, Park K. Oxidative stress induced by cerium oxide nanoparticles in cultured BEAS-2B cells. *Toxicology*. 2008;245:90–100. doi:10.1016/j.tox.2007.12.022
42. Mittal S, Pandey A. Cerium oxide nanoparticles induced toxicity in human lung cells: role of ROS mediated DNA damage and apoptosis. *Biomed Res Int*. 2014;2014:891934. doi:10.1155/2014/891934
43. Kramer J, Minhas N, Jutzeler C, Erskine E, Liu L, Ramer M. Neuropathic pain following traumatic spinal cord injury: models, measurement, and mechanisms. *J Neurosci Res*. 2017;95(6):1295–1306. doi:10.1002/jnr.23881
44. Biurrun Manresa J, Finnerup N, Johannesen I, et al. Central sensitization in spinal cord injured humans assessed by reflex receptive fields. *Clin Neurophysiol*. 2014;125(2):352–362. doi:10.1016/j.clinph.2013.06.186
45. Gaudet A, Fonken L, Ayala M, Maier S, Watkins L. Aging and miR-155 in mice influence survival and neuropathic pain after spinal cord injury. *Brain Behav Immun*. 2021;97:365–370. doi:10.1016/j.bbi.2021.07.003
46. Kobiela Ketz A, Byrnes K, Grunberg N, et al. Characterization of macrophage/microglial activation and effect of photobiomodulation in the spared nerve injury model of neuropathic pain. *Pain Med*. 2017;18(5):932–946. doi:10.1093/pm/pnw144
47. Pannell M, Labuz D, Celik M, et al. Adoptive transfer of M2 macrophages reduces neuropathic pain via opioid peptides. *J Neuroinflammation*. 2016;13(1):262. doi:10.1186/s12974-016-0735-z
48. Zhang Y, Liu J, Wang X, Zhang J, Xie C. Extracellular vesicle-encapsulated microRNA-23a from dorsal root ganglia neurons binds to A20 and promotes inflammatory macrophage polarization following peripheral nerve injury. *Aging*. 2021;13(5):6752–6764. doi:10.18632/aging.202532